Received: 11 July 2021 | Revised: 2 August 2021 | Accepted: 15 August 2021

DOI: 10.1111/all.15091

Allergy EUROPEAN JOURNAL OF ALLERGY AND CLINICAL IMMUNOLOGY EAACI WILEY

ORIGINAL ARTICLE

Allergen-Specific Immunotherapy and Biologics

Development and preclinical evaluation of virus-like particle vaccine against COVID-19 infection

Ismail Cem Yilmaz[1,2] | Emre Mert Ipekoglu[1] | Artun Bulbul[2] | Nilsu Turay[2] | Muzaffer Yildirim[2] | Irem Evcili[2] | Naz Surucu Yilmaz[1] | Nese Guvencli[1] | Yagmur Aydin[1] | Bilgi Gungor[2] | Berfu Saraydar[2] | Asli Gulce Bartan[2] | Bilgehan Ibibik[2] | Tugce Bildik[2] | İlayda Baydemir[1] | Hatice Asena Sanli[1] | Basak Kayaoglu[1] | Yasemin Ceylan[2] | Tugce Yildirim[2] | Irem Abras[2] | Ihsan Cihan Ayanoglu[1] | Sefa Burak Cam[3] | Eda Ciftci Dede[4] | Merve Gizer[5] | Osman Erganis[6] | Fahriye Sarac[7] | Serdar Uzar[7] | Hakan Enul[7] | Cumhur Adiay[7] | Gamze Aykut[2] | Hivda Polat[8] | Ismail Selim Yildirim[8] | Saban Tekin[8] | Gulay Korukluoglu[9] | Hasan Ersin Zeytin[10] | Petek Korkusuz[3] | Ihsan Gursel[2] | Mayda Gursel[1]

[1]Department of Biological Sciences, Middle East Technical University, Ankara, Turkey

[2]Molecular Biology and Genetics Department, Bilkent University, Ankara, Turkey

[3]Hacettepe University Faculty of Medicine Department of Histology and Embryology, Ankara, Turkey

[4]Hacettepe University Graduate School of Science and Engineering, Department of Bioengineering, Ankara, Turkey

[5]Hacettepe University Graduate School of Health Sciences, Department of Stem Cell Sciences, Ankara, Turkey

[6]Faculty of Veterinary Medicine, Selcuk University, Konya, Turkey

[7]Pendik Veterinary Research and Control Institute, Istanbul, Turkey

[8]Marmara Research Center, TUBITAK, Istanbul, Turkey

[9]Virology Laboratory, General Directorate of Public Health, Ankara, Turkey

[10]Biotechnology Research Center, Nobel Pharma, Istanbul, Turkey

Correspondence
Mayda Gursel, Department of Biological Sciences, Middle East Technical University, Ankara, Turkey.
Email: mgursel@metu.edu.tr

Ihsan Gursel, Molecular Biology and Genetics Department, Bilkent University,

Abstract

Background: Vaccines that incorporate multiple SARS-CoV-2 antigens can further broaden the breadth of virus-specific cellular and humoral immunity. This study describes the development and immunogenicity of SARS-CoV-2 VLP vaccine that incorporates the four structural proteins of SARS-CoV-2.

Abbreviations: 2p, 2 proline; 6p, Hexaproline; AFM, atomic force microscopy; Alum, aluminum hydroxide; CD33 SP, cleavable signal peptide; COVID-19, Coronavirus Disease-2019; CpG, cytosine-phosphate-guanine; CT, cytoplasmic tail; CTL, cytotoxic T lymphocyte; E, envelope protein; EC50, half maximal effective concentration; ELISA, enzyme linked immunosorbent assay; FD, T4 fibritin trimerization domain; FP, fusion peptide; GMT, geometric mean titer; GT, Gomori trichrome; H&E, hematoxylin and eosin; hACE2, human angiotensin-converting enzyme 2; HD, high dose; HEK293, human embryonic kidney cell line; His, histidine tag; HR, heptad repeat; IFN-γ, interferon gamma; IL, interleukin; LD, low dose; M, membrane protein; MFI, mean fluorescence intensity; N, nucleocapsid protein; NC, nucleocapsid; NTD, N-terminus domain; ODN, oligodeoxynucleotide; PEIpro, polyethylene imine transfection reagent; Pfu, plaque forming unit; RBD, receptor-binding domain; S, spike protein; SARS-CoV-2, severe acute respiratory syndrome coronavirus 2; SEM, scanning electron microscopy; TEM, transmission electron microscopy; TEV, tobacco etch virus; TH1, T helper 1; TH2, T helper 2; THM, thrombin cleavage site; TM, transmembrane domain; TRPS, tunable-resistive pulse sensing; VAERS, vaccine adverse event reporting system; VLP, virus-like particle; VNT, virus neutralization titer; WT, wild type.

Mayda Gursel and Ihsan Gursel are joint senior authors.

Ankara, Turkey.
Email: ihsangursel@bilkent.edu.tr

Funding information
Turkish Scientific and Research Council

Methods: VLPs were generated in transiently transfected HEK293 cells, purified by multimodal chromatography, and characterized by tunable-resistive pulse sensing, AFM, SEM, and TEM. Immunoblotting studies verified the protein identities of VLPs. Cellular and humoral immune responses of immunized animals demonstrated the immune potency of the formulated VLP vaccine.

Results: Transiently transfected HEK293 cells reproducibly generated vesicular VLPs that were similar in size to and expressing all four structural proteins of SARS-CoV-2. Alum adsorbed, K3-CpG ODN-adjuvanted VLPs elicited high titer anti-S, anti-RBD, anti-N IgG, triggered multifunctional Th1-biased T-cell responses, reduced virus load, and prevented lung pathology upon live virus challenge in vaccinated animals.

Conclusion: These data suggest that VLPs expressing all four structural protein antigens of SARS-CoV-2 are immunogenic and can protect animals from developing COVID-19 infection following vaccination.

KEYWORDS
COVID-19, CpG ODN Adjuvant, SARS-CoV-2, vaccine, virus-like particle

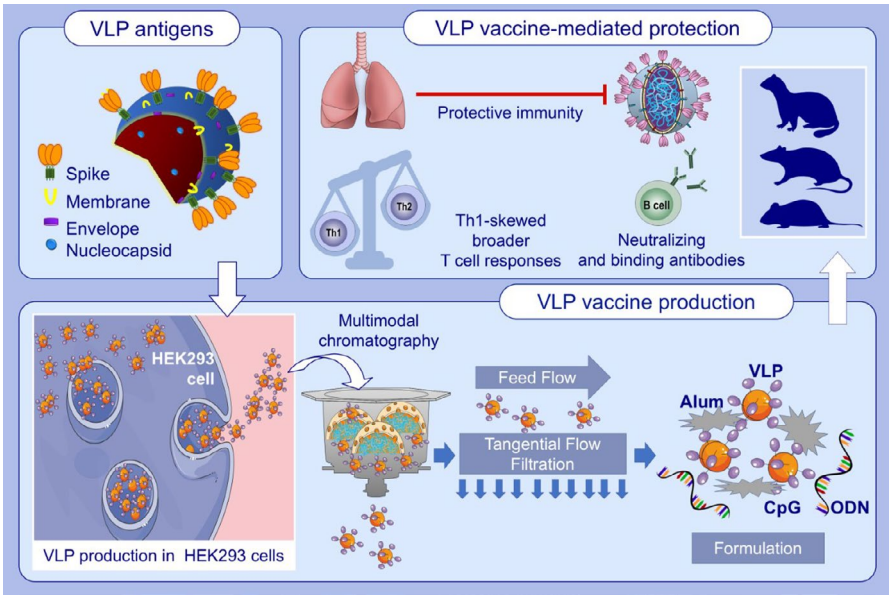

GRAPHICAL ABSTRACT
SARS-CoV-2 VLP vaccine that incorporates the four structural proteins of SARS-CoV-2 is reproducibly produced in suspension adapted HEK293 cells. Alum adsorbed, K3-CpG ODN-adjuvanted VLPs elicit high titer anti-S, anti-RBD, anti-N IgG, and neutralizing antibodies in mice, rats, and ferrets. The VLP vaccine supports multifunctional Th1-biased T-cell responses and demonstrate immunoprotective activity against live SARS-CoV-2 challenge in vaccinated mice.

1 | INTRODUCTION

Rapid development of effective vaccines is indispensable in constraining the COVID-19 pandemic. Multiple highly effective COVID-19 vaccines have recently been approved for human use and several are still in clinical development.[1] The majority of current SARS-CoV-2 vaccines target only the Spike (S) antigen with the main intent of eliciting neutralizing antibodies against the receptor-binding domain (RBD) to neutralize infection.[2-6] However, the emergence of variants of concern Alpha (B.1.1.7), Beta (B.1.351), Gamma (P.1), and Delta (B.1.617.2) with altered S sequences raises concerns on dependence on S-based vaccines, particularly in light of recent evidence indicating the potential for variants to at least partially escape from neutralizing antibodies.[7-18] Although

neutralizing and spike-binding antibodies strongly correlate with protective immune mechanisms,[19] cellular immunity also likely contributes to virus clearance.[20-23] In addition to spike, targeting of other SARS-CoV-2 antigens in vaccines, such as the membrane (M) and nucleocapsid (N), could hypothetically present an advantage over S-dependency of vaccines twofold: First, M and N harbor immunodominant CD4+ and CD8+ T-cell epitopes that can further broaden the breadth of cellular and humoral immunity[24]; second, non-neutralizing anti-N antibodies can potentially contribute to cross-immunity between SARS-CoV-2 variants, akin to heterosubtypic immunity previously reported for influenza viruses.[25,26] In this context, although an inactivated SARS-CoV-2 vaccine would harbor multiple virus antigens, the inactivation process alters the ratio of prefusion form of spike toward its postfusion form, impacting the ability of the vaccine to induce a neutralizing response.[27] To this end, herein, we describe the preclinical development of a virus-like particle (VLP) vaccine expressing the Hexaproline prefusion-stabilized spike (S-6p).[28] To expand the spectrum of ensuing T-cell responses, the VLPs were designed to also express the N, M, and envelope (E) of SARS-CoV-2 structural proteins. To improve immunogenicity, S-6p VLPs were adsorbed to alhydrogel (alum) and formulated with a K-type CpG ODN (also referred to as B type) as a vaccine adjuvant to boost both humoral immunity and cellular (Th1 cells and CTL) immunity.[29-31]

2 | MATERIALS AND METHODS

2.1 | Cloning of VLP encoding genes

Human codon-optimized genes coding for WT, 2p-S, HexaPro spike (6p-S),[27,28] membrane glycoprotein (M) (NCBI Refseq: YP_009724393.1), envelope (E) (NCBI Refseq: YP_009724392.1) and nucleocapsid (N) (NCBI Refseq: YP_009724397.2) proteins of SARS-CoV-2 were synthesized by Integrated DNA Technologies, Inc. with a C- terminus histidine tag. In order to achieve mammalian expression of S, M, E, and N genes, pVitro1 and pVitro2 mammalian dual expression plasmids with different promoters (Invivogen) were used and NEBstable *Escherichia coli* cells were transformed (NEB-C3040). Since BamHI restriction digestion sequence was placed at 5′ and 3′ ends of all synthesized genes, BamHI and BglII cut sites at the multiple cloning sites of both plasmids were used for cloning. The sequences for S (WT, 2p-S, and 6p-S) and E genes were both cloned into the pVitro2 plasmid. While S was cloned at the BamHI restriction site under the human ferritin heavy chain promoter (pVitro2-S), E was cloned by compatible end cloning at the BglII site under the human ferritin light chain promoter (pVitro2-S/E). In parallel, M and N were both cloned into pVitro1. The sequence for M was inserted at the BamHI site under the rat elongation factor 1 alpha (rEF1) promoter (pVitro1-M), while N was cloned at the BglII site under the mouse elongation factor 1 alpha (mEF1) promoter by compatible end cloning (pVitro1-M/N). Plasmid sequences were verified by next-generation sequencing (NGS) (Intergen).

2.2 | Transient transfection of suspension HEK293 cells

HEK293 suspension adapted cell line was purchased from Florabio. Suspension cells were grown in serum and animal protein-free Orchid293 CD transfection media (TFM, Florabio) and supplemented with 400 mg L-glutamine per liter (Sigma). Suspension cells were incubated at 37°C, 8% CO_2 with 130 rpm reciprocal shaking and transiently transfected with PEIpro (Polyplus) during logarithmic growth phase at a cell density of 1.3×10^6/ml. For transient transfection, cell media were replenished by centrifugation at 100 *g* for 5 min. One μg of pVitro1 + pVitro2 mixture was first prepared at a 1.22:1.0, molar ratio per 10^6 cells/ml and was diluted in 5% (v/v) of the final Orchid293 CD TFM volume. The PEIpro/pDNA ratio was optimized as 2:1 (v/w ratio). PEIpro mix was added onto the plasmid DNA mix and vortexed briefly. Following 15 min incubation at RT, the transfection mixture was added dropwise onto cells and gently mixed and incubated for 96–120 h. Culture supernatants then were harvested by centrifugation at 1000 *g* for 10 min and filtered through a 0.22 μm filter membrane (Stericup Quick Release Millipore Express Plus PES filter, Merck Millipore). This solution constituted the secreted extracellular VLPs.

2.3 | Purification of VLPs

To eliminate host cell–derived nucleic acids, the harvest was treated with 200 U/ml of Denarase (c-LEcta) for 2 h at 37°C. VLPs were purified on a Hi-Screen Capto Core 400 (Cytiva) column using ÄKTA-GO fast protein liquid chromatography system (Cytiva). Flow-through fractions containing VLPs were pooled and subjected to ultrafiltration/diafiltration on a Sartocon® Slice 200 Hydrosart® 100 kDA (Sartorius) cassette.

2.4 | SDS-PAGE, Western blotting, and VLP quantification

For SDS-PAGE, the samples were mixed with reducing 4× Laemmli Buffer and denatured at 95°C for 5 min. 18 μl of sample was loaded into each well of 4–20% Mini-PROTEAN TGX Stain-Free Protein Gel (Bio-Rad). Following completion of SDS-PAGE, gels were transferred to a PVDF 0.2 μm membrane using the Mini Trans-Blot® Cell System (Bio-Rad) for an hour at 100 V. As primary antibodies, HRP-conjugated 6xHis, His-Tag antibody (Proteintech), Spike-S1 and Nucleocapsid antibody (ProSci) were used. Anti-rabbit and anti-mouse secondary antibodies were used for anti-spike S1 and anti-N immunoblots. The HRP activity was detected with ECL™ Prime HRP Reagent (Cytiva) and imaged by an Amersham Imager 600 (Cytiva). VLP content was quantified with the Pierce™ micro BCA protein assay kit (Thermo Fisher Scientific) according to manufacturer's instructions.

2.5 | Characterization of VLPs by SEM, AFM, and TEM

A 10 μl of the VLP solution was deposited onto a silica surface, air-dried and sputter-coated with 8 nm of Au/Pd alloy using a precision coating system prior to imaging on an environmental SEM (Technia; FEI).

Purified VLPs were diluted 1:100 in PBS and adsorbed onto mica sheets. The adsorbed samples were air-dried and micrometer-scale AFM imaging was conducted in non-contact dynamic mode (NanoMagnetics Instruments) according to manufacturer's instructions. Scans were analyzed using the NMI Image Analyzer software.

VLP-producing HEK293 cells were processed for standard TEM. Briefly, cells were fixed in 2% glutaraldehyde 30 min at RT, fixed in 1% osmium tetroxide, dehydrated through a graded series of ethanol (30–100%), and embedded in Epon 812 resin. Sections were stained with uranyl acetate and lead citrate. Imaging was performed at 80 kV using a JEOL-JEM 1400 transmission electron microscope. Digital images of the specimens were acquired using a CCD camera (Gatan Inc.).

2.6 | Nanoparticle analysis of VLPs using TRPS

Tunable-resistive pulse sensing (TRPS) measurements were executed with the qNano Gold (IZON S/N 601A) system and analyzed with the IZON Control Suite 3.4.2.48 software (IZON Science LTD). The calibration particles, IZON coating solution, wetting solution, and nanopores were used according to the manufacturer's protocols. 35 μl of 1:1000 diluted calibration particles (CPC100, IZON Reagent Kit, RK3-167) or sample liquid was loaded, and each sample reading was repeated three times.

2.7 | Bead based binding assays

Carboxyl modified latex beads (2 mg of 4% (w/v), Thermo Fisher Scientific) were coated with 5 μg recombinant hACE2 (ProSci) or anti–IL-1β in PBS and blocked in 5% BSA in PBS. Beads were washed once and resuspended in 5% BSA/PBS/0.05% NaN3 (FACS buffer). VLPs were loaded with 50 μM carboxyfluorescein succinimidyl ester (CFSE) for 30 min at 37°C, and free dye was removed using a HiTrap® Desalting column (Cytiva). Recombinant hACE2 and anti–IL1β-coated beads were diluted 1:50. CFSE-labeled VLPs were serially diluted five times; each dilution was mixed with an equal volume of coated bead followed by overnight incubation at 4°C. Beads were washed three times and analyzed on a Novocyte 3000 flow cytometer.

2.8 | Immunization studies

All animal studies were conducted with prior approval of the animal ethics committee of Bilkent University (BIAEC, 2020-7/14.42020) and TUBITAK-MAM ethics committee (Approval No: 16563500-111-60).

VLPs were adsorbed onto 2% Alhydrogel® (10.2 mg/ml, Alum hereafter) and adjuvanted with K3-CpG ODN (2.6 μg/μl). Groups of female mice (BALB/c, C57BL/6, or K18 hACE2 Tg, 6–8 weeks old) were subcutaneously (s.c.) injected with 200 μl VLP vaccine (0.4–24 μg VLP antigen) 2 weeks apart (on 0 and 14 days). Before the day of booster and 2 weeks post-booster injection, mice were bled and sera were stored at −20°C until further use. In some experiments, WT (five mice/group), 2p- (12 mice/group), or 6p-spike expressing VLPs (12 mice/group) were formulated only with Alum (5 μg/mice), or K3-CpG ODN (20μg/mice) or their combinations. In rat (5/group) and ferret (4/group) immunization experiments, 10 or 40 μg VLP adsorbed onto 600 μg Alum and adjuvanted with 300 μg K3-CpG ODN) was s.c. injected 2 weeks apart and blood was collected before the day of booster and 2 weeks post-booster injection. In ED50 experiment, female Balb/C mice (6–8 weeks old, 10/group) were injected with six different doses of VLP (24, 12, 6, 3, 1.5, and 0.75 μg) vaccine containing Alum (30 μg/injection) and K3-CpG ODN (60 μg/injection) on days 0 and 14. Before the day of booster and 2 weeks post-booster injection, mice were bled and sera were collected and stored at −20°C until further use. Extra details were provided in corresponding figure legends.

2.9 | IgG ELISA

Maxi binding semi-hydrophobic enzyme linked immunosorbent assay (ELISA) plates (SPL Life Sciences) were coated with 50 μl/well in-house recombinant 6p-S (5 μg/ml) and nucleocapsid (20 μg/ml), commercial recombinant RBD (3 μg/ml), and inactive SARS-CoV-2 virus (5 μg/ml) in PBS at 4°C overnight. The plates were washed five times (3 min intervals) with PBS-Tween (0.05%, PBS-T) and finally washed with dH_2O and then blocked for 2 h using 200 μl/well 5% BSA-PBS-T solution. Following subsequent washing, 1:50 diluted mice sera were serially diluted fivefold with 5% BSA in PBS-Tween (0.05%, PBS-T) into wells. ALP conjugated anti-mouse IgG (Southern Biotech), anti-mouse IgG1 (Southern Biotech), and anti-mouse IgG2a (Southern Biotech) antibodies were plated at a 1:1000 dilution. For the development of the plates, p-nitrophenyl phosphate (PNPP, Thermo) substrate solution (50 μl/well) was added according to manufacturer's instructions. Consecutive optical density values were measured at 405 nm with a microplate reader (Molecular Devices) for 5 h.

2.10 | Cytometric bead array for measurement of CD4+ helper T responses

CD4+ T helper cell cytokine levels were assessed with the LEGENDplex™ MU Th Cytokine Panel (12-plex) w/ VbP V03 kit (Biolegend) according to the manufacturer's instructions from the supernatants of splenocytes stimulated with nucleocapsid (20 μg/ml) and 6p-Spike proteins (5 μg/ml).

2.11 | SARS-CoV-2 challenge in K18 hACE2 transgenic mice

ACE2 Tg BALB/c mice (6–8 weeks old, 10 mice/group) were immunized twice subcutaneously 14 days apart with low (10 μg) or high (40 μg) dose of VLP + Alum + K3-CpG vaccine or with placebo. On day 36, mice were challenged for three consecutive days with live SARS-CoV-2 virus (10^5 pfu/50 μg; GISIAD gene bank, Accession number ID EPI_ISL_491476, Virus Name: hCoV-19/Turkey/Pen07/2020) intranasally in TUBITAK MAM, BSL3 Animal facility (Ethical Committee Approval No: 16563500-111-60, on 07th/Apr/2021). One week after last virus instillation, animals were sacrificed and major organs were recovered. Viral loads in lung specimens (112 ± 10 mg) were assessed by qRT-PCR using nucleocapsid primers NC1and NC2. Viral RNA was extracted with an the QIAamp Viral RNA Mini kit Cat: 52906 (QIAGEN) according to the protocols. The viral RNA quantification was performed using One Step PrimeScript III RT-qPCR Kit (Takara). All reactions were performed on a CFX96 Touch instrument (BioRad) with the following quantitative-PCR conditions: 52°C for 5 min, 95°C for 10 s, followed by 44 cycles at 95°C for 5 s and 55°C for 30 s. The CDS primer sequences are used for RT-qPCR are targeted against the nucleocapsid (NC) gene of SARS-CoV-2 with the following primers and probes: NC1 Forward: 5′-GAC CCC AAA ATC AGC GAA AT-3′, NC1 Reverse: 5′-TCT GGT TAC TGC CAG TTG AAT CTG-3′, NC1 Probe: 5′-FAM-ACC CCG CAT TAC GTT TGG TGG ACC-BHQ1-3′. NC2 Forward: 5′-TTA CAA ACA TTG GCC GCA AA-3′, NC2 Reverse: 5′-GCG CGA CAT TCC GAA GAA-3′, NC2 Probe: 5′-FAM-ACA ATT TGC CCC CAG CGC TTC AG-BHQ1-3′.

2.12 | Histomorphometric evaluation

Lung samples were fixed in buffered formaldehyde solution. Tissues were dehydrated in an automated tissue processor (TP1020, Leica). Sections were obtained in a temperature-controlled paraffin station (LG1150H-C, Leica) on a sliding microtome (SM2000R, Leica), were deparaffinized at 60°C overnight and stained with Hematoxylin-Eosin and Gomori's Trichrome techniques. All sections were evaluated using a bright field microscope with a camera attachment using an image analysis program (DM6B, DFC7000T, LAS X, Leica). Inflammation was semi-quantitatively scored between 0 and 5 in the perivascular, peribronchiolar, subpleural regions and in the whole section. American Thoracic Society's acute lung injury scoring was followed to report total lung injury.[32] The parenchymal inflammation area was evaluated for each animal by combining the images obtained at 4× magnification using Tile Scanning feature of the analysis program and the area of inflammation was calculated quantitatively in μm^2 and then proportioned to the total lung area.

2.13 | Virus neutralization assay

A micro-neutralization assay was carried out to detect SARS-CoV-2–neutralizing antibodies.[33] The virus used in the authentic Wuhan strain study was isolated in Pendik Veterinary Research and Control Institute (GISIAD gene bank, Accession number ID EPI_ISL_491476, Virus Name: hCoV-19/Turkey/Pen07/2020). Heat-inactivated twofold serially diluted sera were mixed with an equal volume of 100 TCID50 of SARS-CoV-2 for 1 h at 37°C. 100 μl of each dilution was transferred in quadruplicate onto VERO E6 cells (Vero C1008; ATCC No. CRL-1586). After 4 days of incubation, plates were inspected by an inverted optical microscope (Olympus, CKX41). The virus neutralization titers were calculated based on the "Kärber Calculation" as detailed below:

Kärber Calculation: Virus	**Serum**
Titer = L + d(S − 0.5)L = 1st dilution on the plate	**Titer = L + d(S − 0.5)**L = 1st dilution on the plate
D = difference between log dilution steps (0.6)	D = difference between log dilution steps (0.3)
S = sum of wells showing CPE/ total no. of wells per dilution	S = sum of wells showing **no** CPE/total no. of wells per dilution
0.5 = constant	0.5 = constant

Similarly, General Directorate of Public Health Laboratories conducted the Alpha variant VNT assays. The Turkish isolate variant virus strain (hCoV-19/Turkey/HSGM-ES117/2021/EPI_ISL_1938480) was used in these assays. The virus stock was titrated in 96-well microtiter plates on Vero E6 cells in serial log10 dilutions and 10 times for each dilution factor to obtain 50% tissue culture infectious dose (TCID50). The plates were observed for cytopathic effect (CPE) daily for 4 days. The endpoint of viral dilution leading to CPE in 50% of inoculated wells was calculated by using the Reed-Muench method. Both virus titration and MNT were performed in BSL-3 facility. The serum samples were heat-inactivated at 56°C for 30 min. In 96-well microplates, sera were twofold serially diluted in duplicate starting from 1:4 in DMEM supplemented with 2% of heat-inactivated FBS, penicillin, and streptomycin.

100 TCID50 of the hCoV-19/Turkey/HSGM-ES117/2021 strain were added to the serum dilutions and incubated for 1 h at 37°C with 5% CO_2. Vero E6 cells, which were prepared 2×10^5 per ml were added to the virus-serum mix, and plates were incubated for 4 days at 37°C with 5% CO_2. Virus dilution was back titrated in each experiment. Neutralization was assessed by CPE. The complete inhibition of virus propagation in an individual well was accepted as a positive result. The neutralization endpoint titer was determined as the highest serum dilution that inhibited the virus infection in 50% of the inoculated wells (Serum neutralization 50-SN50). The MNT titer ≥4 was considered as positive.

2.14 | Statistical analysis

Statistical differences of all treatment groups were analyzed using Graph Pad Prism 9 statistical software. Groups were compared by one-way ANOVA with Dunnett's multiple comparisons test. Extra comparative statistical analyses were mentioned in the figure legends. In all analyses, a *P* value below .05 was considered to be statistically significant.

3 | RESULTS

3.1 | Expression, purification, and characterization of SARS-CoV-2 VLPs

A panel of spike (S) protein encoding genes (with unmodified and modified versions) of SARS-CoV-2 S, membrane glycoprotein (M), envelope (E), and nucleocapsid (N) were engineered (Figure 1A). Spike genes were designed and synthesized in three forms: WT with unmodified S, 2P with two proline substitutions (K986P and V987P),[34-37] or 6P with six proline substitutions (F817P, A892P, A899P, A942P, K986P, and V987P)[28] to stabilize the prefusion conformation. Modifications made to the polybasic furin cleavage site between S1 and S2, locations of the CD33 signal sequence, T4 fibritin (foldon) trimerization motif and the histidine tag sequence are also indicated in Figure 1A. For the nucleocapsid construct, amino acid sequence of the authentic virus was used without modification. S, M, E, and N genes were codon-optimized for mammalian cells and cloned into pVitro1 (N and M) and pVitro2 (WT, 2P or 6P S, and E) dual mammalian expression plasmids. Transient transfection of pVitro1 and pVitro2 S, M, E, and N-encoding plasmids into HEK293 cells resulted in cellular assembly, secretion, and subsequent accumulation of VLPs in culture supernatant. For the purification of SARS-CoV-2 VLPs (Figure 1B), Denarase treated and clarified cell culture supernatant was loaded onto a HiScreen CaptoCore 400 multimodal size-exclusion/ion-exchange chromatography column and pooled flow-through fraction was subjected to ultrafiltration/diafiltration. VLPs were characterized by transmission electron microscopy (TEM; Figure 1C), scanning electron microscopy (SEM; Figure 1D), atomic force microscopy (AFM; Figure 1E), TRPS (Figure 1F), and immunoblotting for SARS-CoV-2 antigen content using anti-His-Tag, anti-N (Figure 1G), and anti-S1 antibodies (Figure 1H). HEK293 producer cells released intact VLPs into the culture supernatant (Figure 1C). Purified VLPs were spherical, vesicular structures (Figure 1D,E) that were similar in size to SARS-CoV-2 virions (117 ± 38, 127 ± 41, and 119 ± 36 for the WT, 2p or 6p incorporating VLPs, respectively; Figure 1F). Spike protein expression in 2p-VLPs was enhanced relative to WT spike displaying VLPs, whereas 6p-S base construct enabled maximal spike incorporation (Figure 1G). Membrane, envelope, and nucleocapsid expressions were relatively stable and did not change substantially among WT, 2p or 6p spike expressing VLPs (Figure 1G). Comparison of spike-specific immunoblots of 6p-VLPs with inactivated SARS-CoV-2 virions revealed that 6p-VLPs displayed intact full-length spike, whereas a substantial amount of the spike protein generated S1 fragments in the case of inactivated SARS-CoV-2 virions (Figure 1H). 6p-VLPs specifically bound to human ACE2 receptor coated beads but not to anti–IL-1β-coated control beads (Figure S1), demonstrating the specificity of the VLP-expressed spike protein toward the host receptor. The yield of VLPs from one liter harvest was found to be 25 ± 3 mg/L based on microBCA method. Moreover, VLPs retained their intact antigenic content even when incubated at 40°C up to 3 days (Figure S2A), and they retained their morphology after adsorption to alum and CpG adjuvantation (Figure S2B). Furthermore, formulated VLP vaccine was stable for 90 days following storage at 2–8°C and preserved its long-term in vivo immunopotency (Figure S2C). These results illustrate the feasibility of generating VLPs as a vaccine candidate, targeting the four structural proteins of SARS-CoV-2.

3.2 | Immunogenicity of SARS-CoV-2 VLP vaccine

To assess the immunogenicity of the VLP vaccine, 4- to 8-week-old female BALB/c mice were subcutaneously immunized with 0.4 (low dose; LD) and 4 μg (high dose; HD) 2p- or 6p-VLPs, separated by a 2-week interval. VLPs were either administered as such or in combination with K3-CpG (20 μg/mouse), alum (5 μg/mouse), or both. Mice immunized with LD or HD VLP had detectable anti-S-binding IgG and IgG1 after primary (Figure 2A) and booster injections (Figure 2B). As expected, magnitude of the secondary anti-S IgG response in all HD groups was substantially higher than their LD counterparts (5.2-, 12.4-, 12.2-, and 8.5-fold for 6p-VLP, 6p-VLP + K3-CpG, 6p-VLP + Alum, 6p-VLP + K3-CpG + Alum groups, respectively; Figure 2B). 6p-VLP + K3-CpG + Alum elicited 2.7-fold more anti-S IgG when compared to its formulated 2p-VLP counterpart (Figure 2B), indicating that adjuvanted hexaproline stabilized S is more immunogenic than the 2p-stabilized spike containing VLPs. Neither Alum, nor K3-CpG or K3-CpG/Alum combination further elevated anti-S IgG or IgG1 titers. However, contrary to primary response and compared to HD VLP alone, only the K3-CpG-adjuvanted groups elicited significant anti-S IgG2a (13- and ninefold for 6p-VLP HD + K3-CpG and 6p-VLP HD + Alum + K3-CpG when compared to HD 6p-VLP alone group, Figure 2A,B), demonstrating the preferential Th1 skewing immunostimulatory activity of K3-CpG ODN. Similarly, all VLP formulations elicited anti-RBD and anti-N IgG and IgG1 antibodies,

FIGURE 1 Development and characterization of the VLP vaccine. (A) Schematic representation of spike, membrane, envelope, and nucleocapsid protein designs. Included are a cleavable signal peptide (CD33 SP), N-terminal domain (NTD), RBD, S1/S2 boundary (S1/S2), fusion peptide (FP), heptad repeat 1 (HR1), central helix (CH), heptad repeat 2 (HR2), transmembrane domain (TM), cytoplasmic tail (CT), tobacco etch virus protease cleavage site (TEV), T4 fibritin trimerization domain (FD), thrombin cleavage site (THM), and six histidine tag sequence (His). The native polybasic furin cleavage site modifications and proline substitutions to generate the full-length WT, prefusion-stabilized 2p- and 6p-spike variants are also indicated. (B) Schematic representation of VLP production, purification, and formulation process. Representative transmission electron microscopy image of VLP-producing HEK293 cells (C), scanning electron microscopy and atomic force microscopy images of individual VLPs (D) and (E) are shown. (F) TRPS size distribution measurement (nm) of WT, 2p- and 6p-spike variant incorporating VLPs. Analysis of structural proteins assembled into SARS-CoV-2 VLPs by Western blot using anti-His, anti-N (G), and anti-S (H) antibodies

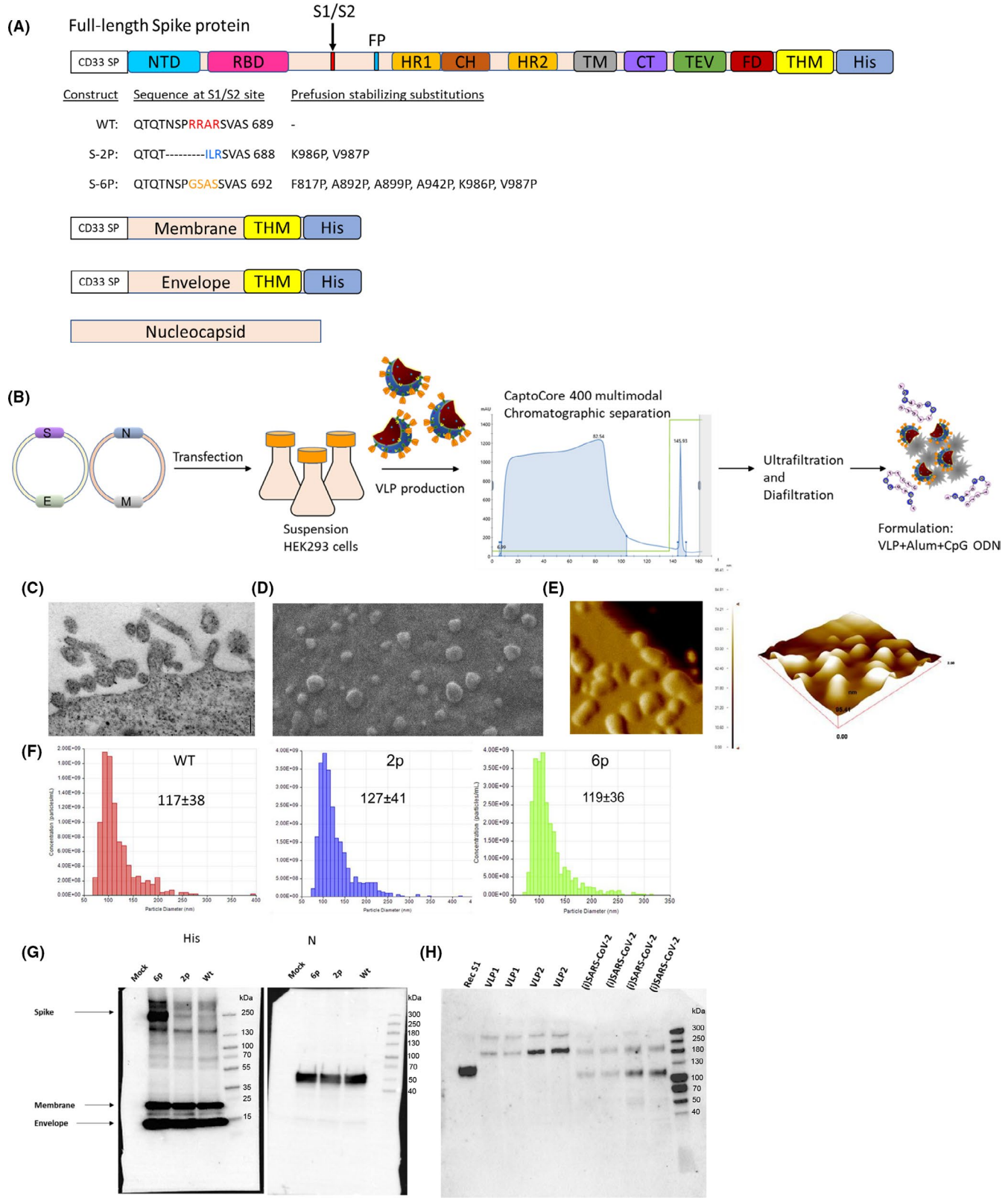

whereas highest anti-RBD and anti-N IgG2a titers were stimulated only in mice immunized with HD VLP plus K3-CpG or CpG/Alum (Figure S3A–D). Although in the BALB/c model IgG1 titers induced by HD 6p-VLP + Alum + K3-CpG well exceeded that of IgG2a, in hACE2 transgenic C57BL/6 mice, the same formulation elicited an anti-RBD IgG2c dominated response (Figure 4A; IgG2c:IgG1 ratio 3:1). Considering the role of IgG2a and/or IgG2c in viral clearance mechanisms,[38-41] K3-CpG ODN adjuvantation confers an advantage over non-adjuvanted and/or Alum adsorbed VLP administration.

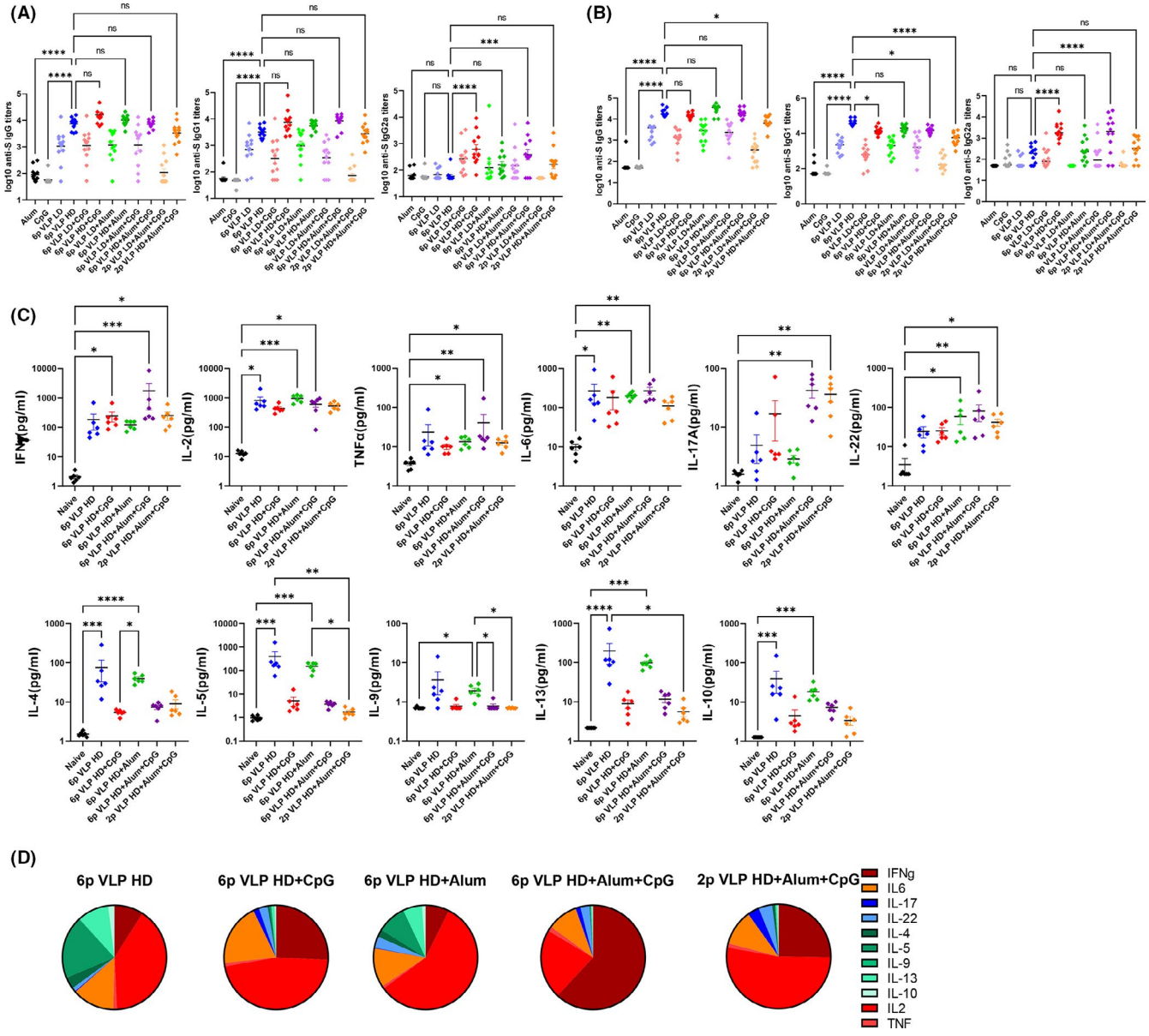

FIGURE 2 VLPs elicit robust antibody and helper T cell responses in mice. BALB/c mice ($n = 12$/group) were immunized on days 0 and 14 with 0.4 μg (low dose; LD) or 4 μg (high dose; HD), 6p-S VLP or 2p-S VLPs without or with Alum (5 μg/mouse), without or with K3 CpG ODN (20 μg/mouse) or with Alum + CpG ODN. Control BALB/c mice were administered Alum or CpG ODN alone (black and gray). Sera were collected 2 weeks post-prime (A) and 2 weeks post-boost (B) and assessed for SARS-CoV-2 S-specific IgG, IgG1, and IgG2a by ELISA. Vaccinated groups were compared by one-way ANOVA with Dunnett's multiple comparisons test. $^{*}P < .05$, $^{**}P < .01$, $^{***}P < .001$, $^{****}P < .0001$. Data are presented as GMT ± geometric SEM. (C) Spleens were collected 2 weeks after booster ($n = 6$). 1×10^{6}/250 μl splenocytes from naive or immunized mice were stimulated with recombinant spike (5 μg/ml) in the presence of 1 μg/ml anti-mouse CD28. T helper cell cytokine levels were assessed from 48 h culture supernatants using the LEGENDplex™ MU Th Cytokine Panel (12-plex). Groups were compared by one-way ANOVA with Dunnett's multiple comparisons test. $^{*}P < .05$, $^{**}P < .01$, $^{***}P < .001$, $^{****}P < .0001$. Data are presented as mean cytokine levels ± SEM. (D) Pie charts representing the proportions of individual secreted S-specific T helper cell cytokines are presented

Antigen-specific helper T-cell responses were also investigated in immunized mice. Following restimulation with recombinant spike or nucleocapsid, splenocytes from mice immunized with 6p-VLP or 6p-VLP plus Alum, secreted significant amounts of Th2 cytokines IL-4, IL-5, IL-13, and IL-10 (Figures 2C,D and S4A,B). In contrast, only the K3-CpG or CpG/Alum-adjuvanted VLPs induced a Th1-biased IFN-γ response but no Th2-associated cytokines (Figures 2C,D and S4A,B), suggesting that 6p-VLP/Alum/K3-CpG vaccination would prevent Th2-biased immune responses and therefore avoid Th2-dependent vaccine-associated enhanced respiratory disease (VAERD).[42-44]

To study the effect of the formulation dose on VLP immunogenicity, BALB/c mice were subcutaneously immunized with six different doses (ranging from 24 to 0.75 μg) of 6p-VLP/Alum/K3-CpG and IgG titers against the whole inactivated virus was determined by ELISA (Figure 3A).

The effective concentration at 50% (EC50) was then determined by a non-linear regression curve fit in GraphPad Prism (Figure 3A). The EC50 for the 6p-VLP/Alum/K3-CpG vaccine was determined to be 2.83 μg.

To test the HD 6p-VLP + Alum + K3-CpG immunogenicity in different animal species, rats were immunized subcutaneously with 40 μg of 6p-VLP/K3-CpG/Alum 2 weeks apart and live virus-neutralizing antibody titers (VNT) were evaluated 2 weeks after booster injection (Figure 3B). Similarly, ferrets were vaccinated either with a 10 μg or a 40 μg dose of the 6p-VLP vaccine and live VNTs were determined 2 weeks after priming and booster injections (Figure 3C). 6p-VLP/Alum/K3-CpG combination induced robust neutralizing antibodies against live SARS-CoV-2 in rats and ferrets. These data indicate that 6p-VLP/Alum/K3-CpG formulation is a potent immunogen that can elicit virus-neutralizing activity in multiple species.

VLPs expressing either WT 6p-S or alpha variant 6p-S were also synthesized and then formulated with alum/CpG ODN to test their immunogenicity in C57BL/6 mice. In alpha 6p-S VLPs, spike protein expression was more enhanced compared to WT 6p-S VLPs (Figure 3D). Consistently, alpha 6p-S VLPs elicited higher levels of anti-S and anti-inactivated virus (Wuhan) IgG in comparison with WT 6p-S VLPs, whereas anti-N IgG levels remained similar (Figure 3E). Antibodies raised against WT, Alpha, Beta, and Gamma variant RBDs were also analyzed (Figure 3F). Alpha 6p-S VLPs elicited ~37.3-, 20.5-, 1.7-, and 11.9-fold more anti-WT, anti-alpha, anti-beta, and anti-gamma RBD IgG, respectively, when compared to WT 6p-S VLP immunized mice (Figure 3F). These results suggest that alpha 6p-S-expressing VLPs might be advantageous over their WT 6p-S VLP counterpart in eliciting a broader cross-protective response against variant RBDs.

3.3 | Protective efficacy of the SARS-CoV-2 VLP vaccine in K18-hACE2 transgenic mice

To evaluate the immunoprotective activity of the 6p-VLP vaccine against challenge with authentic SARS-CoV-2, K18-hACE2 transgenic mice (Jackson Laboratories) were immunized with 8 μg 6p-VLP/Alum/K3-CpG (high dose; HD) on days zero and 14. A low-dose vaccine group (2 μg; low dose; LD) was also included to identify the potential of the VLP vaccine to induce VAERD when suboptimal antibodies are generated. 14 days after booster, mice immunized with the HD VLP

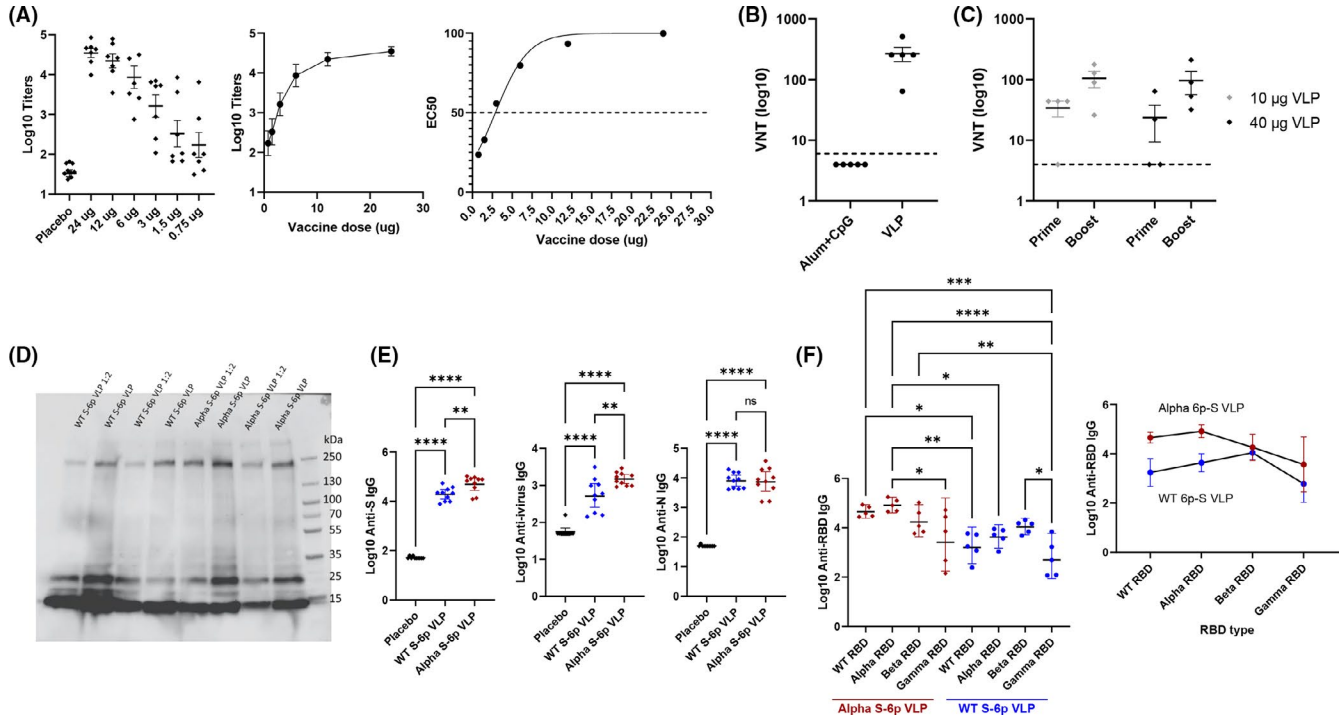

FIGURE 3 Immunogenicity of the VLP vaccine in mice, rats, and ferrets. (A) BALB/c mice (n = 10/group) were subcutaneously immunized with six different doses (24–0.75 μg) of 6p-S VLP/Alum/CpG on days 0 and 14. 2 weeks after the booster injection, IgG titers against the whole inactivated virus was determined by ELISA. ED50 was determined by non-linear regression curve fit in GraphPad Prism. (B) Sprague Dawley rats (n = 5/group) were immunized with 40 μg 6p-S VLP with Alum (600 μg/rat), K3 CpG ODN (300 μg/rat). Live VNTs were evaluated 2 weeks after booster injection. (C) Ferrets (n = 4/group) were vaccinated either with a 10 μg or a 40 μg dose of the VLP with Alum (600 μg/ferret) and K3 CpG ODN (300 μg/ferret). Live VNTs were determined 2 weeks after priming and booster injection. (D) Analysis of spike protein expression in WT 6p or alpha variant 6p-S expressing VLPs by Western blot using anti-His (2.5 μg protein/well; 1:2 indicates twofold diluted sample). (E–F) C57BL/6 mice (n = 5–10/group) were subcutaneously immunized with 8 μg of either WT (five mice/group) 6p-S VLP (10mice/group) or alpha variant 6p-S VLP (10mice/group) vaccine on days 0 and 14. Two weeks after booster injection, (E) S-, inactivated virus- and N-specific IgG titers or (F) WT, alpha, beta, or gamma variant RBD-specific IgG titers were determined by ELISA. Vaccinated groups were compared by one-way ANOVA with Dunnett's multiple comparisons test. *P < .05, **P < .01, ***P < .001, ****P < .0001. Data are presented as GMT ± geometric SEM

vaccine induced significant levels of anti-RBD IgG, IgG1, and IgG2c when compared to placebo group (Figure 4A). In contrast, the LD vaccine generated only low titers of RBD-specific IgG2c (Figure 4A). VNT against original Wuhan or the B.1.1.7 UK variant live viruses was also measured from serum of HD 6p-VLP + Alum + K3-CpG immunized mice, 2 weeks after booster injection (Figure 4B). There was an average of 1.4-fold reduction in VNTs against the more transmissible B.1.1.7 UK variant when compared to the authentic virus, suggesting that the VLP vaccine might be effective against this specific variant of concern.

On day 21 after booster injection, mice were intranasally challenged with 10^5 pfu of live SARS-CoV-2 (Wuhan strain) on 3 consecutive days. One week after the last instillation, lungs were harvested for histopathological evaluation (Figure 4D,E). Histomorphometric evaluations were based on the following criteria: (i) Inflammation was semi-quantitatively scored between 0 and 5 in the perivascular, peribronchiolar, and subpleural regions and in the whole section.[45] (ii) Total lung injury was evaluated based on the American Thoracic Society's acute lung injury score.[32] The parenchymal inflammation area was quantitatively evaluated.[46]

Untreated/unchallenged healthy K18-hACE2 transgenic mouse lung samples (negative control) exhibited low-grade local parenchymal inflammation at the periphery (Figure 4D). Alveolar integrity was preserved without interalveolar septum thickening, intra-alveolar inflammatory cell infiltration, or protein debris accumulation. High-dose vaccine prevented perivascular ($P < .0001$), peribronchiolar ($P = .0002$), subpleural ($P < .0001$), and total ($P < .0001$) lung parenchymal inflammation when compared to the placebo group (Figure 4D,E). Minimal inflammation scores equivalent to healthy animals were recorded in the high-dose vaccine group (Figure 4E).

High-dose vaccine significantly reduced acute lung injury score consisting of inflammatory cell infiltration in the alveolar lumen and interstitial space, hyaline membrane formation, protein debris in the airways, and thickening of the interalveolar septum compared to that of the placebo group (Figure 4D). Lung specimens from animals vaccinated with high-dose VLP had low injury scores similar to healthy lung specimens (Figure 4E). Placebo and low-dose vaccine failed to prevent acute lung injury and presented with parenchymal consolidation with diffuse infiltration of mononuclear cells and macrophages, thickened interalveolar septa to varying degrees, and hyaline membranes at the alveolar walls facing the lumen (Figure 4D). The high-dose vaccine group generally exhibited a limited and mild parenchymal infiltration at peribronchiolar regions.

These results indicate that 6p-VLP vaccination confers immunoprotective activity against SARS-CoV-2 challenge and a suboptimal vaccine dose does not exacerbate virus-induced immunopathology.

4 | DISCUSSION

Several highly effective and safe SARS-CoV-2 vaccines have been approved and are widely administered to the populations of several countries as an indispensable measure in controlling the current pandemic. Almost all of these vaccines are based on the spike antigen and elicit neutralizing antibodies especially against the receptor-binding motif, the least conserved region of the spike antigen. With the emergence of new SARS-CoV-2 variants of concern and in light of evidence of reduced neutralization activity against some of the VOCs, vaccines that incorporate multiple antigens that are not under selective antibody pressure, could in theory contribute to long-term protective immunity through expanding the breadth of virus-specific T-cell responses.

In this respect, herein, we described the development and immunogenicity of SARS-CoV-2 VLP vaccine that incorporates the four structural proteins of the virus, all of which possess T-cell epitopes.[24-26,47,48]

Our results showed that HEK-293 cells transfected with SARS-CoV-2 structural proteins reproducibly generated VLPs that were similar in size and physical form to the authentic virus. VLPs expressing the hexaproline stabilized prefusion spike antigen adjuvanted with Alum plus K3 CpG ODN elicited high levels of anti-S, anti-RBD, anti-N IgG, and live virus-neutralizing antibodies in mice, rats, and ferrets. Of note, only the CpG ODN-adjuvanted groups induced IgG2a in immunized BALB/c mice, consistent with an immune response characterized by CpG ODN-mediated Th1-type cytokines.[49] Similarly, only the CpG or CpG/Alum-adjuvanted VLP vaccine triggered S- and N-specific Th1- but not Th2-dominated cytokine secretion from T cells. Vaccine adjuvants are of utmost importance in enhancing and directing the adaptative immune response to protein antigens. The widely used vaccine adjuvant alum has a strong Th2 bias. CpG ODN aids in re-directing alum-induced strong Th2 responses toward the Th1 axis.[50] Differently, following injection, CpG ODN adjuvants locate less efficiently to draining lymph nodes in species larger than mice.[51] This drawback can be overcome through formulating the antigen and K3-CpG ODN together with alum to facilitate their delivery to lymph nodes.[52]Our data also indicate that VLPs expressing hexaproline stabilized alpha variant spike elicited a more potent response against WT and variant RBDs compared to 6p-WT S incorporating VLPs. Whether this is due to enhanced spike expression in VLPs or a change in immunogenicity of the variant spike, remains to be determined.

A comparison of protective efficacies of seven SARS-CoV-2–specific vaccines (mRNA-1273, NVX-CoV2373, BNT162b2, rAd26-S+rAd5-S, ChAdOx1 nCoV-19, Ad26.COV2.S, and CoronaVac) from various clinical trials revealed that neutralizing antibody titers were highly predictive of immune protection. Interestingly, three of the vaccines that induced the strongest neutralizing antibody titers and the highest protective efficacy (mRNA-1273, NVX-CoV2373, and BNT162b2) are those that incorporated the prefusion-stabilized form of spike in their design, whereas the CoronaVac vaccine in which the inactivation process most likely generates postfusion spike conformation[27] was found to be the least protective.[53] In this respect, inclusion of the super-stable hexaproline spike and other structural proteins of SARS-CoV-2 in the vaccine design could hypothetically provide an advantage over certain vaccines (ie, inactivated) in terms of humoral immunity and in general, would aid to broaden the breadth of T-cell responses.

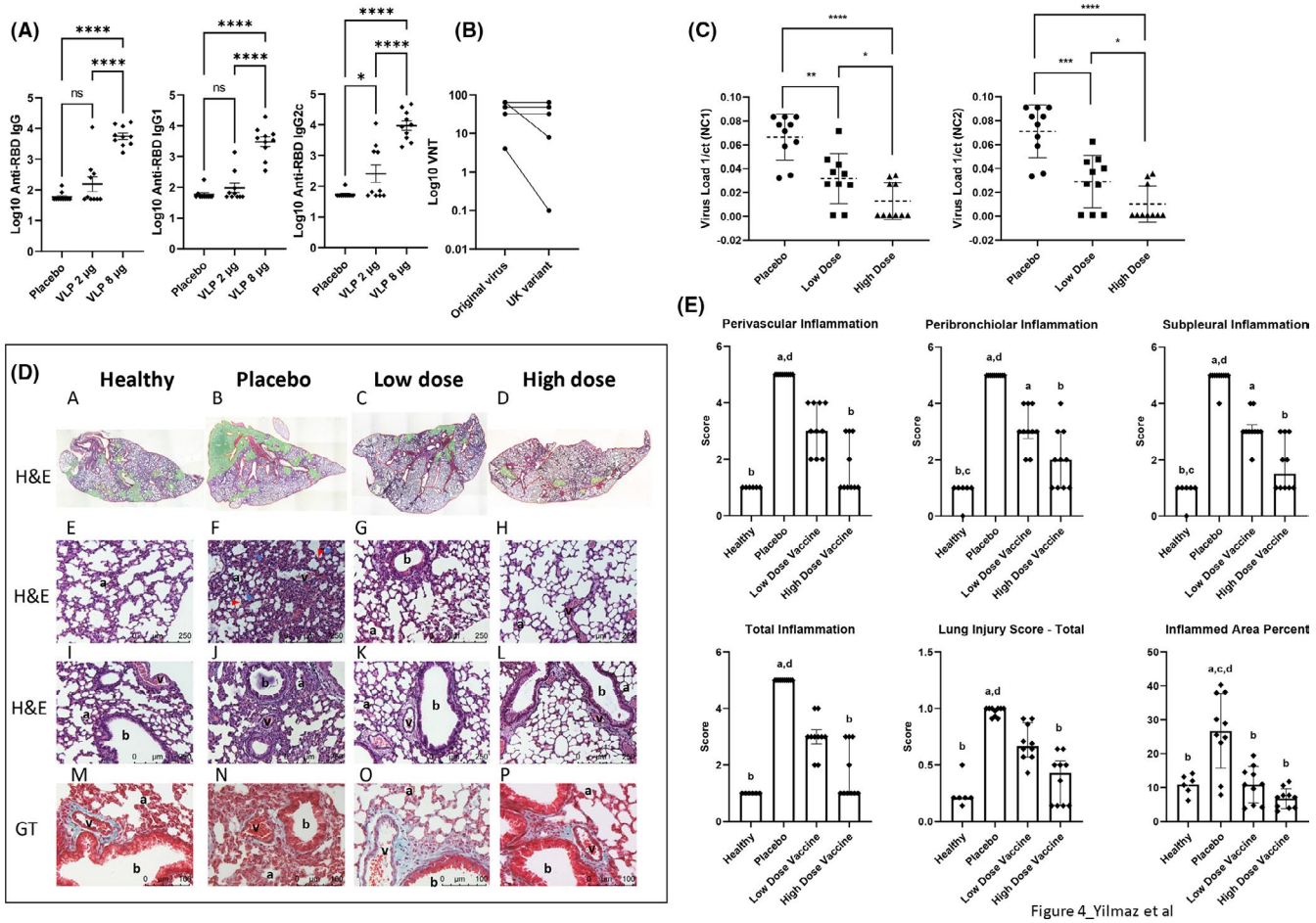

FIGURE 4 Immunoprotective activity of the VLP vaccine in K18-hACE2 transgenic mice. K18-hACE2 transgenic mice ($n = 10$/group) were subcutaneously immunized with 2 µg (low dose; LD) or 8 µg (high dose; HD) of the VLP vaccine on days 0 and 14. Two weeks after booster injection, (A) RBD-specific IgG, IgG1, IgG2c antibody titers were determined by ELISA and (B) neutralizing antibody titers against the authentic Wuhan strain and the B.1.1.7. Alpha variant were determined. Groups were compared by one-way ANOVA with Dunnett's multiple comparisons test. $^{*}P < .05$, $^{**}P < .01$, $^{***}P < .001$, $^{****}P < .0001$. On day 21 after booster, mice were challenged intranasally on 3 consecutive days with 50 µl of 1×10^5 pfu/mouse of SARS-CoV-2 (Wuhan strain). Lungs were collected 7 days after last virus instillation. (C) Infectious virus loads in lung homogenates were assessed by qRT-PCR against the nucleocapsid (NC1 and NC2). Bars represent the mean virus load ($n = 10$/group) as 1/ct values. Comparisons were performed by unpaired Student's t test; $^{*}P < .05$, $^{**}P < .01$, $^{***}P < .001$, $^{****}P < .0001$. (D) Histological micrographs showing healthy (first column), placebo (second column), low-dose vaccine (third column), and high-dose vaccine (fourth column) groups. (A–D) Hematoxylin-eosin (H&E), areas marked green shows inflamed parts of the lungs; (E–L) H&E, 20×; M-P, Gomori Trichrome (GT), 40×. a, alveoli; b, bronchiole; v, blood vessel; blue arrow, protein debris; red arrow, hyaline membrane. (E) Histomorphometric measurements. The descriptive statistics were presented as median and interquartile range in all graphs except for inflamed area percent (mean ± SD). Statistical significance ($P < .05$): a, compared to healthy group; b, compared to placebo group; c, compared to low-dose vaccine group, d, compared to high-dose vaccine group. Nonparametric variables were compared between groups using Kruskal-Wallis test. Pairwise comparisons were made with Dunn's test. Parametric variables were compared in multiple groups using one-way analysis of variance. Pairwise comparisons were performed with the Tukey test

In summary, based on the immunogenicity data presented herein, the CpG ODN/alum-adjuvanted 6p-VLP vaccine (VLP-58-1023-Al-K3) is currently being evaluated in a phase 1 human clinical trial (NCT04818281).

ACKNOWLEDGEMENTS

This work is supported by TUBITAK, Center of Excellence Support Program (1004 Program) to MG as part of the consortium titled "Development of Drug and Vaccine against COVID-19" (Project No: 18AG020). IG received partial support from Ministry of Development (Grant name: UMRAM-ASI, Project #: 2015BSV302). The authors would like to thank, Nobel Pharma Biotechnology Research Center Team heads and all their team members, particularly to Mohan Babu Kasa, Mohit Sharma, Naidu Mookala, Vivek Yadav, and Tirumal Rao Yannabathina. We sincerely appreciate the encouragement and support from Prof Hasan Mandal, and Minister Mustafa Varank.

CONFLICT OF INTEREST

There is no financial conflict of interest to declare by the Authors.

AUTHOR CONTRIBUTIONS

ICY, MG, and IG conceptualized the project. MG and IG led the study. These authors acted as co-second authors: EMI, AB, NT, NSY, NG, MY, and IE. ICY designed protocols and carried out experiments together with BG, BS, TB, YA, IB, AGB, BI, HAS, BK, YC, TY, IA, ICA, and GA. Under the supervision of PK, SBC, ECD, and MG, conducted histopathological investigations and performed TEM analyses. OE provided inactivated SARS-CoV-2 virus samples. FC supervised VNT assays and carried out experiments together with SU, HE, CA. GK carried out alpha variant specific VNT assay. Challenge experiments were supervised by ST and carried out by HP and ISY. HEZ coordinated the GMP production of VLPs in Nobel Pharma. MG and IG wrote the manuscript with input from all authors.

ORCID

Emre Mert Ipekoglu https://orcid.org/0000-0003-3104-7509
Artun Bulbul https://orcid.org/0000-0003-1301-8368
Nilsu Turay https://orcid.org/0000-0002-6365-3469
Eda Ciftci Dede https://orcid.org/0000-0001-6900-4702
Merve Gizer https://orcid.org/0000-0003-1911-2363
Serdar Uzar https://orcid.org/0000-0002-0120-7148
Cumhur Adiay https://orcid.org/0000-0001-6230-6425
Saban Tekin https://orcid.org/0000-0003-2641-6293
Petek Korkusuz https://orcid.org/0000-0002-7553-3915
Ihsan Gursel https://orcid.org/0000-0003-3761-1166
Mayda Gursel https://orcid.org/0000-0003-0044-9054

REFERENCES

1. McGill COVID19 Vaccine Tracker Team, COVID19 Vaccine Tracker. https://covid19.trackvaccines.org/vaccines/
2. Baden LR, El Sahly HM, Essink B, et al. Efficacy and safety of the mRNA-1273 SARS-CoV-2 vaccine. *N Engl J Med*. 2021;384(5):403-416. 10.1056/NEJMoa2035389
3. Polack FP, Thomas SJ, Kitchin N, et al. Safety and efficacy of the BNT162b2 mRNA Covid-19 vaccine. *N Engl J Med*. 2020;383(27):2603-2615. 10.1056/NEJMoa2034577
4. Voysey M, Clemens SAC, Madhi SA, et al. Safety and efficacy of the ChAdOx1 nCoV-19 vaccine (AZD1222) against SARS-CoV-2: an interim analysis of four randomised controlled trials in Brazil, South Africa, and the UK. *Lancet*. 2021;397(10269):99-111. 10.1016/S0140-6736(20)32661-1
5. Logunov DY, Dolzhikova IV, Shcheblyakov DV, et al. Safety and efficacy of an rAd26 and rAd5 vector-based heterologous prime-boost COVID-19 vaccine: an interim analysis of a randomised controlled phase 3 trial in Russia. *Lancet*. 2021;397(10275):671-681. 10.1016/S0140-6736(21)00234-8
6. Sadoff J, Gray G, Vandebosch AN, et al. Safety and efficacy of single-dose Ad26.COV2.S vaccine against Covid-19. *N Engl J Med*. 2021;384(23):2187-2201. 10.1056/NEJMoa2101544
7. Hoffmann M, Arora P, Groß R, et al. SARS-CoV-2 variants B.1.351 and P.1 escape from neutralizing antibodies. *Cell*. 2021;184(9):2384-2393.e12. 10.1016/j.cell.2021.03.036
8. Tada T, Dcosta BM, Samanovic-Golden M, et al. Neutralization of viruses with European, South African, and United States SARS-CoV-2 variant spike proteins by convalescent sera and BNT162b2 mRNA vaccine-elicited antibodies. *bioRxiv*. 2021. 10.1101/2021.02.05.430003
9. Garcia-Beltran WF, Lam EC, St. Denis K, et al. Multiple SARS-CoV-2 variants escape neutralization by vaccine-induced humoral immunity. *Cell*. 2021;184(9):2372-2383.e9. 10.1016/j.cell.2021.03.013
10. Ikegame S, Siddiquey MNA, Hung CT, et al. Qualitatively distinct modes of Sputnik V vaccine-neutralization escape by SARS-CoV-2 Spike variants. *medRxiv*. 2021. 10.1101/2021.03.31.21254660
11. McCallum M, Bassi J, De Marco A, et al. SARS-CoV-2 immune evasion by the B.1.427/B.1.429 variant of concern. *Science*. 2021;373:648-654. 10.1126/science.abi7994
12. Cele S, Gazy I, Jackson L, et al. Escape of SARS-CoV-2 501Y.V2 from neutralization by convalescent plasma. *Nature*. 2021;593(7857):142-146. 10.1038/s41586-021-03471-w
13. Madhi SA, Baillie V, Cutland CL, et al. Efficacy of the ChAdOx1 nCoV-19 Covid-19 vaccine against the B.1.351 variant. *N Engl J Med*. 2021;384(20):1885-1898. 10.1056/NEJMoa2102214
14. Emary KRW, Golubchik T, Aley PK, et al. Efficacy of ChAdOx1 nCoV-19 (AZD1222) vaccine against SARS-CoV-2 variant of concern 202012/01 (B.1.1.7): an exploratory analysis of a randomised controlled trial. *Lancet*. 2021;397(10282):1351-1362. 10.1016/S0140-6736(21)00628-0
15. Zhou D, Dejnirattisai W, Supasa P, et al. Evidence of escape of SARS-CoV-2 variant B.1.351 from natural and vaccine-induced sera. *Cell*. 2021;184(9):2348-2361.e6. 10.1016/j.cell.2021.02.037
16. Kustin T, Harel N, Finkel U, et al. Evidence for increased breakthrough rates of SARS-CoV-2 variants of concern in BNT162b2-mRNA-vaccinated individuals. *Nat Med*. 2021;27:1379-1384. 10.1038/s41591-021-01413-7
17. Davis C, Logan N, Tyson G, et al. Reduced neutralisation of the Delta (B.1.617.2) SARS-CoV-2 variant of concern following vaccination. *medRxiv* 2021. 10.1101/2021.06.23.21259327
18. Liu C, Ginn HM, Dejnirattisai W, et al. Reduced neutralization of SARS-CoV-2 B.1.617 by vaccine and convalescent serum. *Cell*. 2021;184:4220-4236.e13. 10.1016/j.cell.2021.06.020
19. Earle KA, Ambrosino DM, Fiore-Gartland A, et al. Evidence for antibody as a protective correlate for COVID-19 vaccines. *Vaccine*. 2021;39:4423-4428. 10.1016/j.vaccine.2021.05.063
20. Peng Y, Mentzer AJ, Liu G, et al. Broad and strong memory CD4+ and CD8+ T cells induced by SARS-CoV-2 in UK convalescent individuals following COVID-19. *Nat Immunol*. 2020;21(11):1336-1345. 10.1038/s41590-020-0782-6
21. Rydyznski Moderbacher C, Ramirez SI, Dan JM, et al. Antigen-specific adaptive immunity to SARS-CoV-2 in acute COVID-19 and associations with age and disease severity. *Cell*. 2020;183(4):996-1012.e19. 10.1016/j.cell.2020.09.038
22. Mathew D, Giles JR, Baxter AE, et al. Deep immune profiling of COVID-19 patients reveals distinct immunotypes with therapeutic implications.*Science*. 2020;369(6508):eabc8511. 10.1126/science.abc8511
23. Sekine T, Perez-Potti A, Rivera-Ballesteros O, et al. Robust T cell immunity in convalescent individuals with asymptomatic or mild COVID-19. *Cell*. 2020;183(1):158-168.e14. 10.1016/j.cell.2020.08.017
24. Grifoni A, Weiskopf D, Ramirez SI, et al. Targets of T cell responses to SARS-CoV-2 Coronavirus in humans with COVID-19 disease and unexposed individuals. *Cell*. 2020;181(7):1489-1501.e15. 10.1016/j.cell.2020.05.015
25. Carragher DM, Kaminski DA, Moquin A, Hartson L, Randall TD. A novel role for non-neutralizing antibodies against nucleoprotein in facilitating resistance to influenza virus. *J Immunol*. 2008;181(6):4168-4176. 10.4049/jimmunol.181.6.4168
26. Caddy SL, Vaysburd M, Papa G, et al. Viral nucleoprotein antibodies activate TRIM21 and induce T cell immunity. *EMBO J*. 2021;40(5):e106228. 10.15252/embj.2020106228

27. Ke Z, Oton J, Qu K, et al. Structures and distributions of SARS-CoV-2 spike proteins on intact virions. *Nature*. 2020;588(7838):498-502. 10.1038/s41586-020-2665-2
28. Hsieh C-L, Goldsmith JA, Schaub JM, et al. Structure-based design of prefusion-stabilized SARS-CoV-2 spikes. *Science*. 2020;369(6510):1501-1505. 10.1126/science.abd0826
29. Scheiermann J, Klinman DM. Clinical evaluation of CpG oligonucleotides as adjuvants for vaccines targeting infectious diseases and cancer. *Vaccine*. 2014;32(48):6377-6389. 10.1016/j.vaccine.2014.06.065
30. Shirota H, Klinman DM. Recent progress concerning CpG DNA and its use as a vaccine adjuvant. *Expert Rev Vaccines*. 2014;13(2):299-312. 10.1586/14760584.2014.863715
31. Ezoe S, Palacpac NMQ, Tetsutani K, et al. First-in-human randomised trial and follow-up study of *Plasmodium falciparum* blood-stage malaria vaccine BK-SE36 with CpG-ODN(K3). *Vaccine*. 2020;38(46):7246-7257. 10.1016/j.vaccine.2020.09.056
32. Matute-Bello G, Downey G, Moore BB, et al. An official American Thoracic Society workshop report: features and measurements of experimental acute lung injury in animals. *Am J Respir Cell Mol Biol*. 2011;44(5):725-738. 10.1165/rcmb.2009-0210ST
33. Gu H, Chen Q, Yang G, et al. Adaptation of SARS-CoV-2 in BALB/c mice for testing vaccine efficacy. *Science*. 2020;369(6511):1603-1607. 10.1126/science.abc4730
34. Corbett KS, Edwards DK, Leist SR, et al. SARS-CoV-2 mRNA vaccine design enabled by prototype pathogen preparedness. *Nature*. 2020;586(7830):567-571. 10.1038/s41586-020-2622-0
35. Pallesen J, Wang N, Corbett KS, et al. Immunogenicity and structures of a rationally designed prefusion MERS-CoV spike antigen. *Proc Natl Acad Sci USA*. 2017;114(35):E7348-E7357. 10.1073/pnas.1707304114
36. Wrapp D, Wang N, Corbett KS, et al. Cryo-EM structure of the 2019-nCoV spike in the prefusion conformation. *Science* 2020;367(6483):1260-1263. 10.1126/science.abb2507
37. Walls AC, Park YJ, Tortorici MA, Wall A, McGuire AT, Veesler D. Structure, function, and antigenicity of the SARS-CoV-2 spike glycoprotein. *Cell*. 2020;181(2):281-292.e6. 10.1016/j.cell.2020.02.058
38. Huber VC, McKeon RM, Brackin MN, et al. Distinct contributions of vaccine-induced immunoglobulin G1 (IgG1) and IgG2a antibodies to protective immunity against influenza. *Clin Vaccine Immunol*. 2006;13(9):981-990. 10.1128/CVI.00156-06
39. Huber VC, Lynch JM, Bucher DJ, Le J, Metzger DW. Fc receptor-mediated phagocytosis makes a significant contribution to clearance of influenza virus infections. *J Immunol*. 2001;166(12):7381-7388. 10.4049/jimmunol.166.12.7381
40. Mozdzanowska K, Feng J, Eid M, Zharikova D, Gerhard W. Enhancement of neutralizing activity of influenza virus-specific antibodies by serum components. *Virology*. 2006;352(2):418-426. 10.1016/j.virol.2006.05.008
41. Jayasekera JP, Moseman EA, Carroll MC. Natural antibody and complement mediate neutralization of influenza virus in the absence of prior immunity. *J Virol*. 2007;81(7):3487-3494. 10.1128/JVI.02128-06
42. Kim HW, Canchola JG, Brandt CD, et al. Respiratory syncytial virus disease in infants despite prior administration of antigenic inactivated vaccine. *Am J Epidemiol*. 1969;89(4):422-434. 10.1093/oxfordjournals.aje.a120955
43. Bolles M, Deming D, Long K, et al. A double-inactivated severe acute respiratory syndrome coronavirus vaccine provides incomplete protection in mice and induces increased eosinophilic proinflammatory pulmonary response upon challenge. *J Virol*. 2011;85(23):12201-12215. 10.1128/JVI.06048-11
44. Czub M, Weingartl H, Czub S, He R, Cao J. Evaluation of modified vaccinia virus Ankara based recombinant SARS vaccine in ferrets. *Vaccine*. 2005;23(17–18):2273-2279. 10.1016/j.vaccine.2005.01.033
45. Tian JH, Patel N, Haupt R, et al. SARS-CoV-2 spike glycoprotein vaccine candidate NVX-CoV2373 immunogenicity in baboons and protection in mice. *Nat Commun*. 2021;12(1):372. 10.1038/s41467-020-20653-8
46. Han K, Blair RV, Iwanaga N, et al. Lung expression of human angiotensin-converting enzyme 2 sensitizes the mouse to SARS-CoV-2 infection. *Am J Respir Cell Mol Biol*. 2021;64(1):79-88. 10.1165/rcmb.2020-0354OC
47. Meyers LM, Gutiérrez AH, Boyle CM, et al. Highly conserved, non-human-like, and cross-reactive SARS-CoV-2 T cell epitopes for COVID-19 vaccine design and validation. *NPJ Vaccines*. 2021;6(1):71. 10.1038/s41541-021-00331-6
48. Matchett WE, Joag V, Stolley JM, et al. Nucleocapsid vaccine elicits spike-independent SARS-CoV-2 protective immunity. *J Immunol*. 2021;207(2):376-379. 10.4049/jimmunol.2100421
49. Klinman DM, Klaschik S, Sato T, Tross D. CpG oligonucleotides as adjuvants for vaccines targeting infectious diseases. *Adv Drug Deliv Rev*. 2009;61(3):248-255. 10.1016/j.addr.2008.12.012
50. Weeratna RD, Brazolot Millan CL, McCluskie MJ, Davis HL. CpG ODN can re-direct the Th bias of established Th2 immune responses in adult and young mice. *FEMS Immunol Med Microbiol*. 2001;32(1):65-71. 10.1111/j.1574-695X.2001.tb00535.x
51. Davis HL. Novel vaccines and adjuvant systems: the utility of animal models for predicting immunogenicity in humans. *Hum Vaccin*. 2008;4(3):246-250. 10.4161/hv.4.3.5318
52. Lopez AM, Hecker R, Mutwiri G, van Drunen Littel-van den Hurk S, Babiuk LA, Townsend H. Formulation with CpG ODN enhances antibody responses to an equine influenza virus vaccine. *Vet Immunol Immunopathol*. 2006;114(1–2):103-110. 10.1016/j.vetimm.2006.07.013
53. Khoury DS, Cromer D, Reynaldi A, et al. Neutralizing antibody levels are highly predictive of immune protection from symptomatic SARS-CoV-2 infection. *Nat Med*. 2021;27(7):1205-1211. 10.1038/s41591-021-01377-8

SUPPORTING INFORMATION

Additional supporting information may be found in the online version of the article at the publisher's website.

How to cite this article: Yilmaz IC, Ipekoglu EM, Bulbul A, et al. Development and preclinical evaluation of virus-like particle vaccine against COVID-19 infection. *Allergy*. 2021;00:1–13. https://doi.org/10.1111/all.15091